Supplemental Data

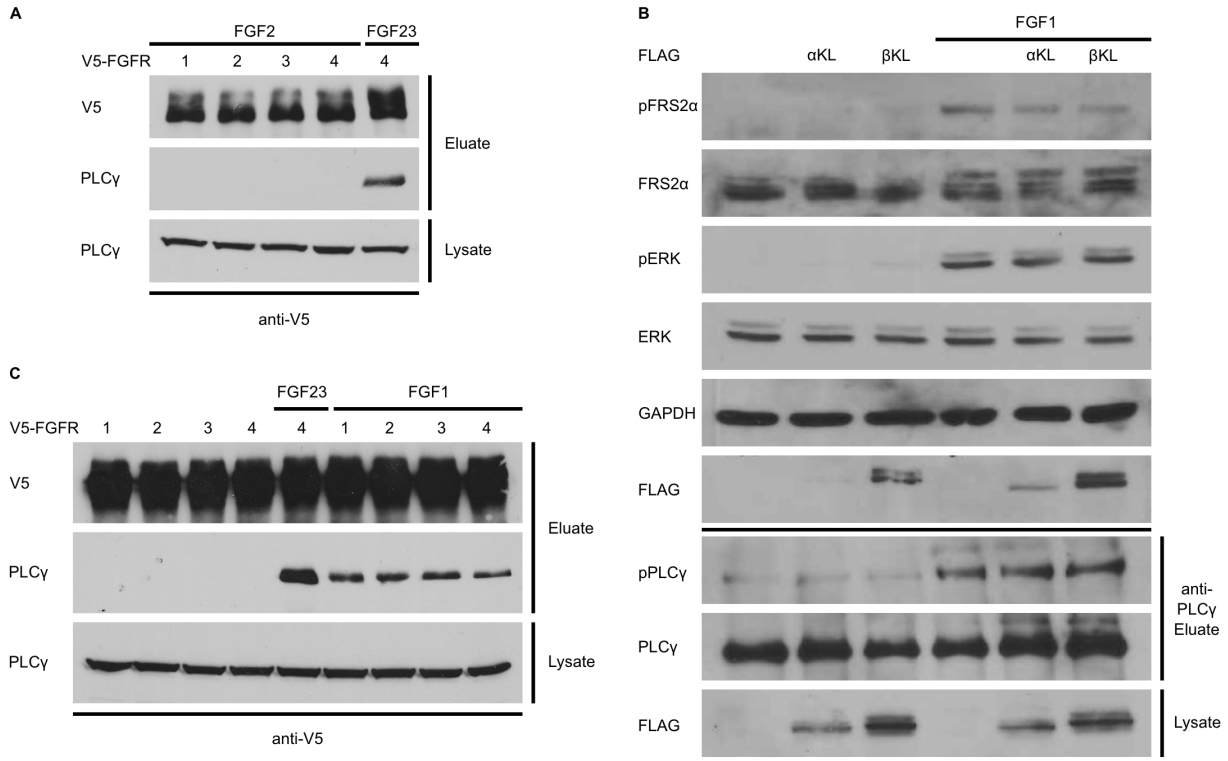

Figure S1, related to Figure 1. FGF1, but not FGF2, activates PLCγ signaling in HEK293 cells.

(**A**) The four different FGFR isoforms (c splice variants of FGFR1-3) were overexpressed as V5-tagged fusion proteins in HEK293 cells for 2 days, serum starved overnight and treated with FGF2 or FGF23 at 25 ng/ml for 30 minutes followed by anti-V5 immunoprecipitation from total protein extracts. In the presence of FGF23 endogenous PLCγ co-precipitates with FGFR4. In contrast, FGF2 treatment does not induce binding of PLCγ to FGFR1, FGFR2, FGFR3 or FGFR4. This assay confirms that FGF2 does not active PLCγ in HEK293 cells. (**B**) Since several studies have shown that FGF1-mediated FGFR activation can induce phosphorylation and thereby activation of PLCγ in different cell types (Burgess et al., 1990; Mohammadi et al., 1996;

Mohammadi et al., 1992; Peters et al., 1992; Wang et al., 1994), we tested if FGF1 has similar effects in HEK293 cells. FGF1 treatment for 30 minutes increases endogenous levels of phosphorylated FRS2α and ERK1/2, as revealed by Western blot analysis of total protein extracts. FGF1 also elevates phosphorylation of immunoprecipitated PLCγ. Overexpression of FLAG-tagged α-klotho (αKL) or β-klotho (βKL) does not alter the effect of FGF1 on the phosphorylation of FRS2α, ERK1/2 or PLCγ. Ectopic α- and β-klotho do not induce phosphorylation of FRS2α, ERK1/2 or PLCγ in the absence of FGF1 treatment. GAPDH serves as loading control. This experiment indicates that in HEK293 cells, FGF1 activates Ras/MAPK as well as PLCγ signaling, and as expected from FGF1's action as a paracrine growth factor, these effects are not altered in the presence of klotho co-receptors. (**C**) HEK293 cells overexpressing the four different V5-tagged FGFR isoforms were serum starved overnight and treated with FGF1 or FGF23 at 25 ng/ml for 30 minutes followed by anti-V5 immunoprecipitation. Treatment with FGF1 induces binding of endogenous PLCγ to ectopic FGFR1, FGFR2, FGFR3 and FGFR4. In the absence of FGF treatment, none of the four FGFR isoforms co-precipitate PLCγ. In the presence of FGF23, PLCγ binds to FGFR4. This experiments indicates that FGF1 induces PLCγ binding to all four FGFR isoforms, which is in line with other studies showing that FGF1 can activate PLCγ via different FGFR isoforms (Chen et al., 2005; Kanai et al., 1997; Mohammadi et al., 1992; Vainikka et al., 1994; Vainikka et al., 1992).

A

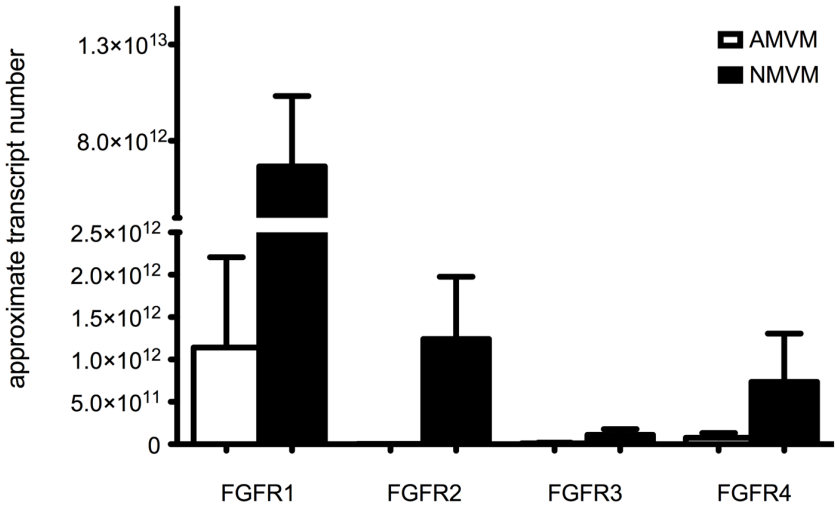
AMVM
NMVM
approximate transcript number
1.3×10^13
8.0×10^12
2.5×10^12
2.0×10^12
1.5×10^12
1.0×10^12
5.0×10^11
0
FGFR1
FGFR2
FGFR3
FGFR4

B

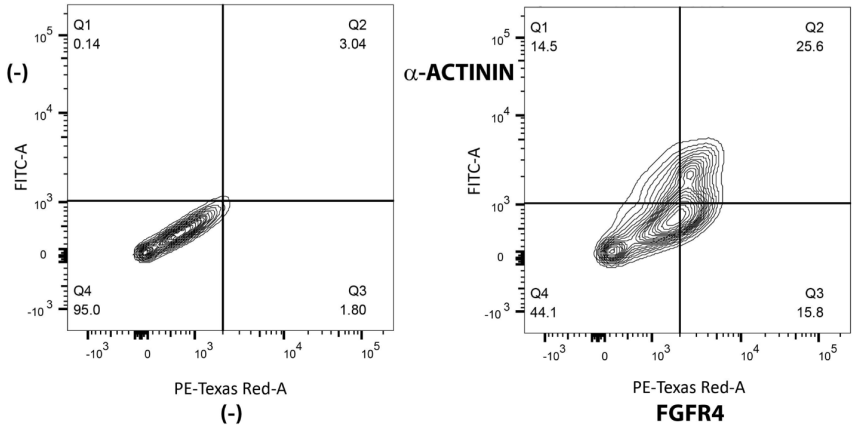
(-)
Q1
0.14
Q2
3.04
Q4
95.0
Q3
1.80
FITC-A
PE-Texas Red-A
(-)
α-ACTININ
Q1
14.5
Q2
25.6
Q4
44.1
Q3
15.8
FITC-A
PE-Texas Red-A
FGFR4

C

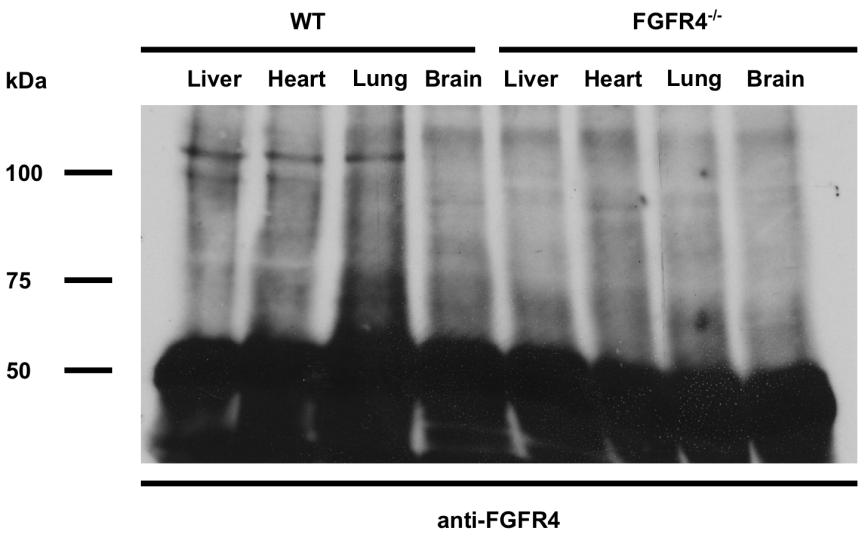
WT
FGFR4-/-
kDa
Liver
Heart
Lung
Brain
Liver
Heart
Lung
Brain
100
75
50
anti-FGFR4

Figure S2, related to Figure 2. FGFR4 is expressed in different tissues.

(**A**) Quantitative PCR analysis of isolated neonatal and adult ventricular myocytes (NMVM and AMVM) for the expression of the four FGFR isoforms. No significant differences in FGFR4 expression levels can be detected between both groups (n = 3 independent isolations). This analysis indicates that of the four FGFR isoform, FGFR1 shows highest expression levels in primary cardiac myocyte cultures. Furthermore, cardiac myocytes from newborn as well as adult mice both express FGFR4 at similar levels. Expression of FGFR2 and FGFR3 were only detectable in cardiac myocytes from newborn mice. (**B**) Representative contour plots of 3 independent flow cytometric analyses of total cardiac cell populations from adult wild-type mouse hearts. Labeling without primary antibodies is used as negative control (-). Numbers refer to percentages of quadrant analysis. FGFR4 is present in α-actinin-positive myocytes, whereas α-actinin-negative non-myocytes show much less FGFR4 labeling. This outcome is similar to the result from the FGFR4/troponin T flow cytometry study, thereby confirming that cardiac myocytes express FGFR4. **(C)** Immunoprecipitation of FGFR4 from total tissue extracts of adult wild-type (WT) and FGFR4 knock-out (*FGFR4*$^{-/-}$) mice followed by immunoblotting for FGFR4 reveals the expected 110 kDa signal of FGFR4 in liver, heart and lung that is absent from *FGFR4*$^{-/-}$ mice. FGFR4 is not detectable in total brain extracts. The 50 kDa signal is the IgG heavy chain of anti-FGFR4. This finding shows that FGFR4 is expressed in several different but not all mouse tissues. This immunoprecipitation assay with isoform-specific anti-FGFR4 antibodies using global FGFR4 knock-out mice as negative control, can serve as an experimental approach to screen for FGFR4 expression.

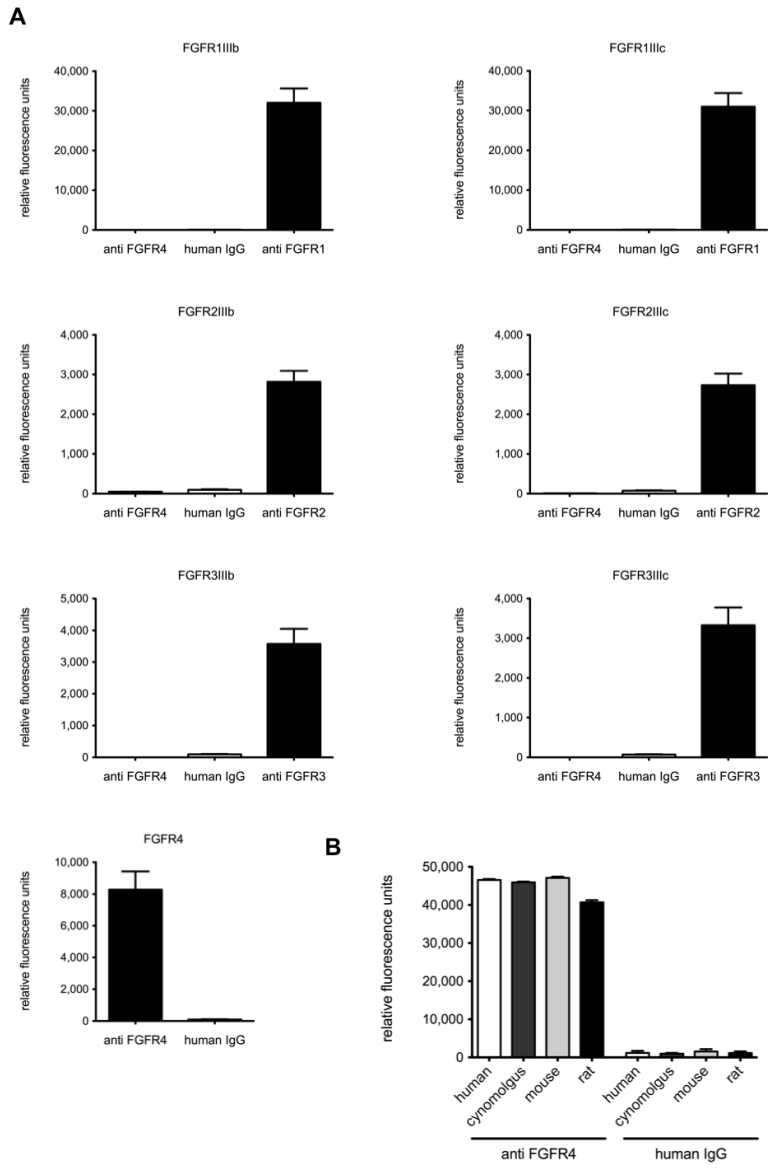

Figure S3, related to Figure 3. Among the FGFR isoforms, anti-FGFR4 only binds FGFR4. (**A**) Analysis of anti-FGFR4 binding to the extracellular domains of different FGFR isoforms and splice variants by ELISA reveals that anti-FGFR4 only binds to FGFR4. Human IgG serves as negative control and antibodies against FGFR1, FGFR2 and FGFR3 as positive controls for binding to respective FGFR isoforms (n = 3 independent experiments with each experiment conducted in triplicates). (**B**) ELISA for anti-FGFR4 binding to the extracellular FGFR4 domain from different species (representative experiment from n = 3, each in triplicates).

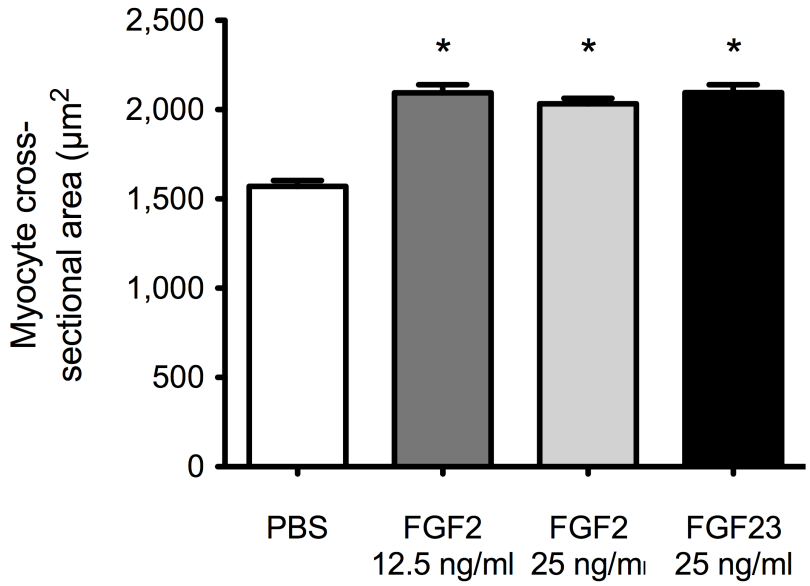

Figure S4, related to Figure 3. FGF2 and FGF23 induce hypertrophic growth of isolated cardiac myoyctes at same molar concentrations.

We repeated the cross-sectional area analyses in isolated NRVM using FGF2 and FGF23 at the same molar concentration, i.e. 0.75 nM (FGF2 at 12.5 ng/ml, and FGF23 at 25 ng/ml). Compared with PBS-treated control cells, 48 hours of treatment with FGF2 or FGF23 at these concentrations significantly increases cross-sectional area of NRVM (mean ± SEM). FGF2 effects were not different when compared to FGF2 treatment with the higher dose of 25 ng/ml (or 1.5 nM) that is used throughout our manuscript. (150 cells per condition; $n = 3$ independent isolations of NRVM; $*P < 0.0001$ compared with vehicle).

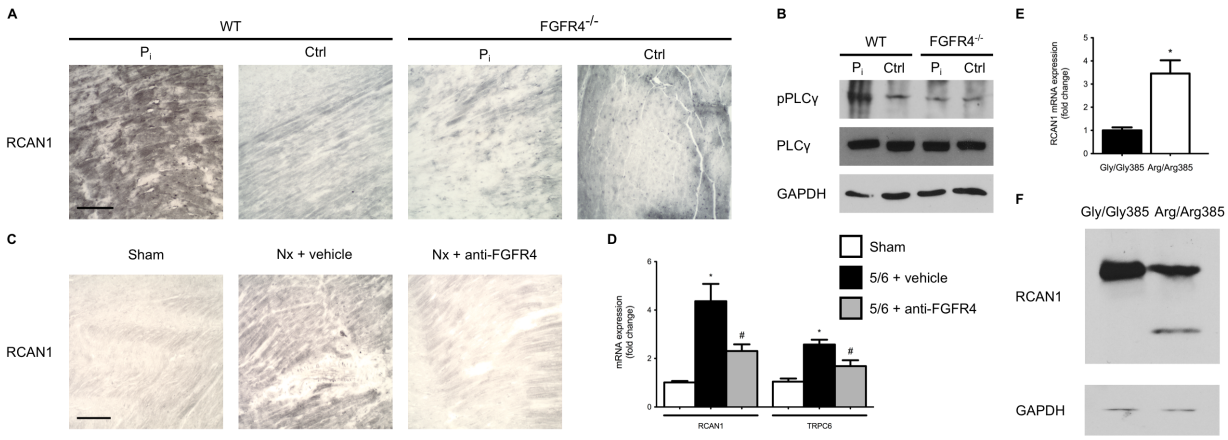

Figure S5, related to Figures 5-7. FGFR4 mediates cardiac PLCγ/calcineurin/NFAT signaling in rodents.

(**A**) Representative immunoperoxidase labeling of mid-chamber sections of the heart demonstrate increased expression of RCAN1 in wild-type mice on high phosphate diet (P_i). *FGFR4*$^{-/-}$ mice on high phosphate or wild-type and *FGFR4*$^{-/-}$ mice on normal diet (Ctrl) show no elevations in RCAN1 levels. (**B**) Western blot analysis of total cardiac extracts shows that high phosphate diet increases levels of phosphorylated PLCγ (pPLCγ) in wild-type mice, but not in *FGFR4*$^{-/-}$ mice. Total PLCγ levels are not altered among groups. GAPDH shows equal protein loading. (**C**) Representative immunoperoxidase labeling of mid-chamber sections of the heart show increased expression of RCAN1 in 5/6 nephrectomy (Nx) rats treated with vehicle compared to sham rats or 5/6 nephrectomy rats that were treated with an FGFR4-specific blocking antibody (anti-FGFR4). (**D**) Quantitative PCR analysis of cardiac tissue shows that expression levels of NFAT target genes, RCAN1 and TRPC6, are significantly elevated in 5/6 nephrectomy rats that were treated with vehicle but not in anti-FGFR4 treated rats (n = 6 rats per group; $^{*}P < 0.001$ compared with Sham; $^{\#}P < 0.05$ compared with Nx + vehicle). (**E**) Quantitative PCR analysis of total hearts from mice reveals significantly elevated RCAN1 expression in 6-month old *FGFR4Arg/Arg385* mice compared with wild-type (n = 6 mice per

group; *$P < 0.01$). (**F**) Western blot analysis of total hearts demonstrates that the NFAT-regulated RCAN1-4 isoform (28 kDa, lower band) can be detected only in *FGFR4Arg/Arg385* but not in wild-type mice. The upper band is the NFAT-independent RCAN1-1 isoform (38 kDa) that is detected in both mouse lines. GAPDH shows equal protein loading.

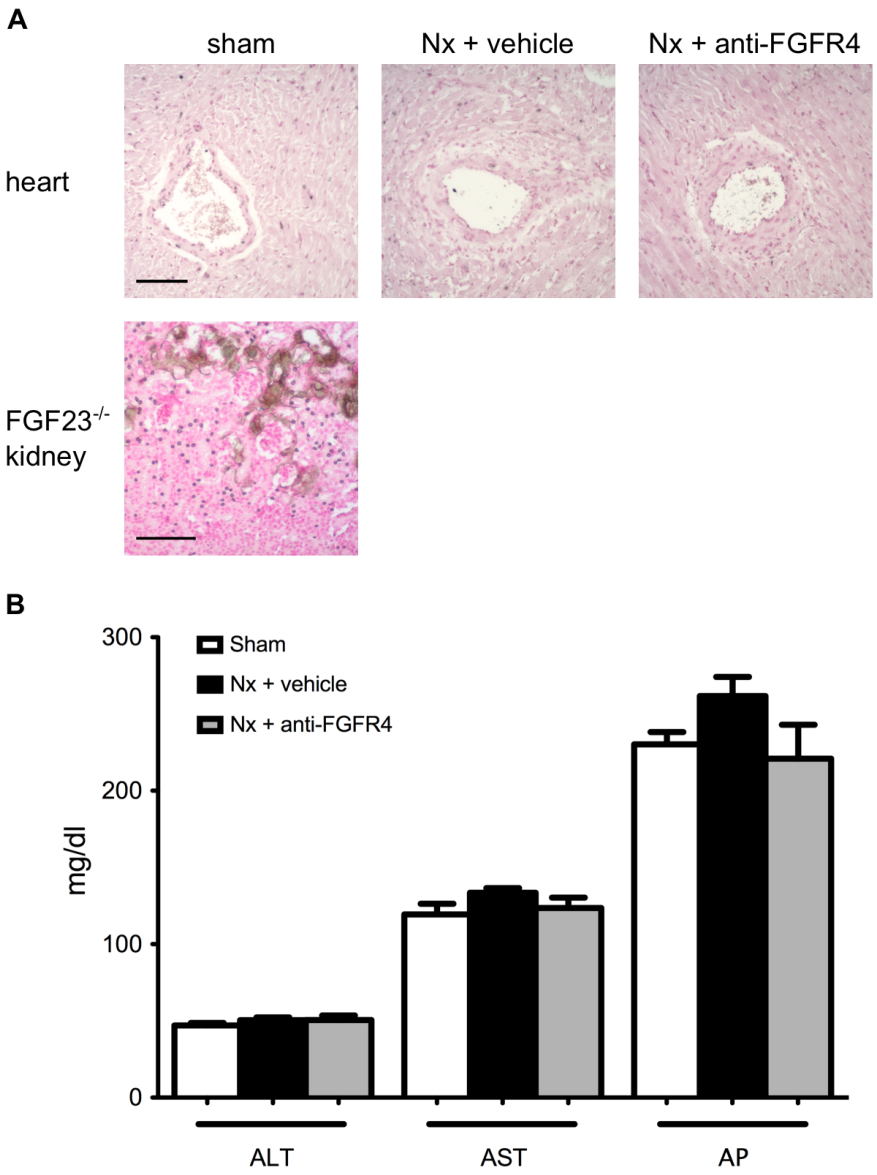

Figure S6, related to Figure 6.

(A) Representative van Kossa stainings from the left ventricular mid-chamber of rats at day 14 after 5/6 nephrectomy (Nx) (original magnification, ×20; scale bar: 100 µm), and from kidney cortex of global FGF23-/- mice (original magnification, ×20; scale bar: 100 µm). Dark staining indicates van Kossa positive mineralization in the FGF23-/- kidney that is not detected around cardiac vessels or in the myocardium of 5/6 nephrectomized rats that received anti-FGFR4. This

finding indicates that anti-FGFR4 treatment does not induce vascular calcification. (**B**) ELISA from serum samples derived from 5/6 nephrectomized (Nx) rats derived 2 weeks post surgery. Rats were administered an FGFR4-specific blocking antibody (anti-FGFR4) or vehicle (PBS) starting 1 hour post surgery. Compared with sham nephrectomy and 5/6Nx rats that were injected with PBS, anti-FGFR4 in 5/6Nx does not significantly alter serum levels of alanine aminotransferase (ALT), aspartate aminotransferase (AST) or alkaline phosphatase (AP) (n = 6-14 rats per group). This finding indicates hat anti-FGFR4 treatment (at least at this particular time-course and delivery dose) does not induce liver injury.

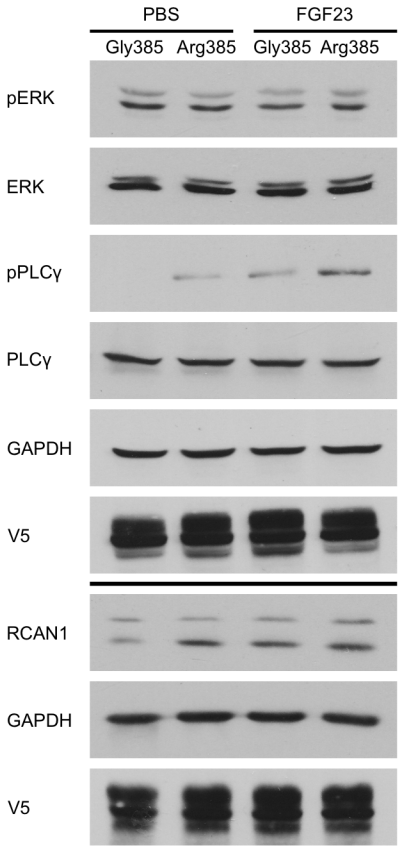

Figure S7, related to Figure 7. Expression of FGFR4Arg385 in HEK293 cells induces activation of calcineurin/NFAT signaling.

As revealed by Western blot analysis of total protein extracts, overexpression of V5-tagged *FGFR4Arg385* in HEK293 cells increases PLCγ phosphorylation and RCAN1-4 expression compared to HEK293 cells that overexpress wild-type *FGFR4Gly385*. The lower band in RCAN1 blots is the NFAT-regulated RCAN1-4 isoform (28 kDa); the upper band is the NFAT-independent RCAN1-1 isoform (38 kDa). FGF23 treatment increases levels of phospho-PLCγ within 30 minutes and RCAN1-4 within 6 hours in HEK293 cells that express wild-type FGFR4. FGF23 further elevates phospho-PLCγ in *FGFR4Arg385* cells. Overexpression of *FGFR4Arg385* or treatment with FGF23 does not increase ERK1/2 phosphorylation. GAPDH shows equal protein loading.

Table S1, related to Figure 6. Pharmacological inhibition of FGFR4 does not improve kidney function or blood pressure in 5/6 nephrectomized rats.

	Sham	**5/6Nx + Vehicle**	**5/6Nx + anti-FGFR4**
Systolic blood pressure (mmHg)	143 ± 5	215 ± 7[A]	211 ± 6[A,B]
Diastolic blood pressure (mmHg)	101 ± 6	168 ± 10[A]	162 ± 8[A,B]
Serum creatinine (mg/dl)	0.23 ± 0.01	0.78 ± 0.09[A]	0.67 ± 0.1[A,B]
Blood urea nitrogen (mg/dl)	15 ± 1	43 ± 7[A]	41 ± 5[A,B]
Creatinine clearance (ml/min/100g)	0.78 ± 0.04	0.24 ± 0.02[A]	0.33 ± 0.05[A,B]
Serum phosphate (mg/dl)	7.0 ± 0.2	6.5 ± 0.5	7.0 ± 0.5[B]
Serum FGF23 (pg/ml)	140 ± 3	495 ± 154[A]	237 ± 44[A,B]

Compared with sham nephrectomy, 5/6 nephrectomy (Nx) in rats results in impaired renal function, hypertension, and elevated serum FGF23 levels that are not significantly changed by delivery of a specific anti-FGFR4 antibody. Values are reported as mean ± SEM; $^{A}P < 0.05$ compared with sham; $^{B}P > 0.05$ compared with 5/6Nx + vehicle.

Table S2, related to Experimental Procedure. Nucleotide sequences of primers that were used in this study.

ANP	rat	forward	AAATCCCGTATACAGTGCGG
		reverse	GGAGGCATGACCTCATCTTC
ANP	rat (NRVM)	forward	ACCTGCTAGACCACCTGGAGG
		reverse	GCTGTTATCTTCCGTACCGG
BNP	mouse	forward	TGGGAGGTCACTCCTATCCT
		reverse	GGCCATTTCCTCCGACTTT
BNP	rat	forward	CCAGAACAATCCACGATGC
		reverse	TCGAAGTCTCTCCTGGATCC
BNP	rat (NRVM)	forward	GCAGCATGGATCTCCAGAAGG
		reverse	CTGCAGCCAGGAGGTCTTCC
aMHC	rat	forward	GAGCAGGAGCTGATCGAGAC
		reverse	CCTCTGCGTTCCTACACTCC
bMHC	rat	forward	CTCCAGAAGAGAAGAACTCC
		reverse	CCACCTGCTGGACATTCTGC
RCAN1	mouse	forward	GCTTGACTGAGAGAGCGAGTC
		reverse	CCACACAAGCAATCAGGGAGC
RCAN1	rat	forward	CTCACACACGTGGACCACCA
		reverse	CGCCCAATCCAGACAAACAG
TRPC6	rat	forward	TCCCCTTCGTTCACTTCATC
		reverse	GACAGAAATCAGCTGGCACA
Fibronectin	mouse	forward	AGACCATACCTGCCGAATGTAG

		reverse	GAGAGCTTCCTGTCCTGTAGAG
Fibronectin	rat	forward	GCCGCAGACCTGGGGCTGCTG
		reverse	CGGCATGAAGCATTCAATTGGG
Col1a2	mouse	forward	AGCAGGTCCTTGGAAACCTT
		reverse	AGGGAGTTTCATCTGGCCCT
Col5a1	mouse	forward	CTACATCCGTGCCCTGGT
		reverse	CCAGCACCGTCTTCTGGTAG
Col1a1	rat	forward	GGTCCTGCTGGTGAGAGAGGT
		reverse	GGCACCAAGGTCTCCAGGAAC
Col3a1	rat	forward	TGCCACCCTGAACTCAAGAGCG
		reverse	CGCGGGACAGTCATGGGACTG
Periostin	mouse	forward	GAACGAATCATTACAGGTCCTG
		reverse	CCTTGGAGACCTCTTTTTGCAAGA
Timp1	mouse	forward	CTGCTCAGCAAAGAGCTTTC
		reverse	CTCCAGTTTGCAAGGGATAG
Timp1	rat	forward	CACTGCCTGCAGCTTCCTGGT
		reverse	GGGATGGCTGAACAGGGAAAC
GAPDH	mouse	forward	CCCATGTTTGTGATGGGTGT
		reverse	GAGCTTCCCGTTCAGCTCT
GAPDH	rat	forward	CATCAACGACCCCTTCATTGAC
		reverse	ACTCCACGACATACTCAGCACC
beta actin	rat	forward	ATGGATGACGATATCGCTGCGC
		reverse	TCAGGGTCAGGATGCCTCTCTT

18S rRNA	rat	forward	TCAAGAACGAAAGTCGGAGG
		reverse	GGACATCTAAGGGCATCAC

All primers are presented in 5’-3’ orientation and used for SYBR Green qPCR analyses.

Supplemental Experimental Procedure

Anti-FGFR4 blocking antibody

Fully human anti-FGFR4 (U3-11) was isolated by U3 Pharma/Daiichi-Sankyo in a phage display screen using the n-CoDeR^{TM} library from Bioinvent, Sweden. The binding of anti-FGFR4 against the extracellular domain of different FGFR isoforms as well as the extracellular domain of FGFR4 from different species (human, mouse, rat and cynomolgus monkey) was determined by ELISA. 0.5 μg of designated, recombinant FGFR was added into each well of a MaxiSorp flat-bottom 96 well ELISA plate (Sigma-Aldrich) and incubated at 4°C overnight. The next day, the solution was removed and 250 μl PBS containing 0.5% BSA was added to each well and incubated for 1 hour at room temperature. After blocking, plates were washed with 200 μl PBS/0.05% Tween per well and cycle for a total of 5 cycles. Anti-FGFR4, antibodies against FGFR1, FGFR2, or FGFR3 (Santa Cruz) or human IgG control was added at a concentration of 10 μg/ml in PBS containing 0.5% BSA (100 μl volume per well). Following 1 hour incubation at room temperature, plates were washed and binding was detected using alkaline phosphatase-conjugated secondary antibodies (anti human IgG F(ab')2 AP (goat) for anti-FGFR4 and human IgG control or anti-rabbit IgG AP (goat) for designated receptor specific antibodies). The secondary antibodies were incubated in PBS containing 0.5% BSA at room temperature for 1 hour. After a final wash, enzyme activity was detected with the AttoPhos AP Fluorescent Substrate System and measured on the Fluostar Omega fluorescent plate reader instrument from BMG Labtech (Ortenberg; Germany). Recorded values were exported, and blank values subtracted from all other values and plotted using Graph Pad Prism.

Growth Factors

We used recombinant mouse FGF23 (6His-tagged Tyr25-Val251 [Arg179Gln]; 26.1 kDa), and FGF2 (Ala11-Ser154; 16.2 kDa) (R&D Systems) as before (Faul et al., 2011). We confirmed in vitro biological activity of FGF23 by detecting increased levels of phospho-ERK1/2 and Egr-1 in response to treatment with FGF23 in HEK293 cells that transiently express FLAG-tagged α-klotho (Kurosu et al., 2006). We confirmed in vivo biological activity of FGF23 by demonstrating significantly decreased serum phosphate levels over 4 hours after a single intravenous injection of 40 μg/kg of purified protein dissolved in 0.5 ml of PBS in 3 male Sprague Dawley rats (Charles River).

Plasmid constructs

We sub-cloned full-length mouse α- and β-klotho cDNAs from pEF1 (provided by Makoto Kuro-o; University of Texas Southwestern, Dallas, TX (Kurosu et al., 2006)) into pFLAG-CMV-5c (Sigma-Aldrich). V5-epitope tagged FGFR cDNA constructs in pcDNA3.1(+) were obtained from Makoto Kuro-o (Kurosu et al., 2006). We used full-length mouse cDNAs for FGFR1c, FGFR2c, FGFR3c and FGFR4. We created the G385R and Y751F variants of mouse FGFR4 using the QuikChange II Site-Directed Mutagenesis Kit (Agilent Technologies). All constructs were verified by DNA sequencing.

HEK293 cell culture and transient transfections

HEK293 cells were grown in 6-well plates or 10 cm-culture dishes and transiently transfected with FuGene 6 (Roche) according to the manufacturer's protocol. After 36 hours, cells were

serum-starved for 12-16 hours followed by treatment with FGF23 or FGF2 at 25 ng/ml for 15 or 30 minutes.

Isolation and culture of NRVM

NRVM were isolated using a standard isolation system (Worthington Biochemical Corporation) (Faul et al., 2011). Hearts from 1-2 day old Sprague Dawley rats were harvested, minced in calcium- and magnesium-free Hank's Balanced Salt Solution (HBSS), and the tissue digested with 50 μg/ml trypsin at 4°C for 20-24 hours. Soybean trypsin inhibitor in HBSS was added, and the tissue was further digested with collagenase (in Leibovitz L-15 medium) under slow rotation (15 rpm) at 37°C for 45 minutes. Cells were released by triturating the suspension 20 times with a standard 10 ml plastic serological pipette and filtering it twice through a cell strainer (70 μm, BD Falcon). Cells were incubated at room temperature for 20 minutes and spun at 100 g for 5 minutes. The cell pellet was resuspended in plating medium [Dulbecco's Modified Eagle Medium (DMEM; Cellgro) with 17% Media 199 (Invitrogen), 15% fetal bovine serum (FBS; Invitrogen) and 1% penicillin/streptomycin solution (P/S; Invitrogen)]. Cells were counted using a hemocytometer.

Cells were plated on glass and plastic surfaces, which were coated with laminin (Invitrogen; 10 μg/ml in PBS) at room temperature for 1 hour prior to plating. For immunofluorescence analysis, 3 x 10^5 cells were seeded per well on glass coverslips in 24-well plates. For Western blot or qPCR analyses of total extracts, 1 x 10^6 cells were seeded per well in 6-well plates, and for immunoprecipitation assays, 5 x 10^6 cells were seeded in 10 cm-culture dishes. Cells were left undisturbed in plating medium at 37°C for 72 hours and then cultured in maintenance medium (DMEM with 20% Media 199, 1% insulin-transferrin-sodium selenite

solution [ITS; Sigma-Aldrich] and 1% P/S) in the presence of 100 μM 5-bromo-2'-deoxyuridine (BrdU; Sigam-Aldrich). After 4 days, isolated cardiac myocytes were cultured in BrdU-containing maintenance medium in the presence of recombinant murine FGF23 or FGF2 (both at 25 ng/ml) for different time points.

Isolation and culture of NMVM

NMVM were isolated enzymatically (Kreusser et al., 2014). Briefly, hearts from 1-3 day-old mice were harvested, minced in PBS/glucose and further digested with collagenase type 2 (0.2% w/v) and DNase (0.05% w/v) on a rotary shaker at 37°C for 11 minutes. Cells were then released from the tissue by triturating the suspension twice with a standard 10 ml plastic serological pipette, transferred to DF10 medium (Dulbecco's Modified Eagle Medium/ Ham's Nutrient Mixture F12 adjusted to 17 mM $NaHCO_2$ containing 2mM L-glutamine, 1% P/S and 10% FBS), and stored on ice. The remaining tissue was further incubated in PBS/glucose/collagenase/DNase solution on a rotary shaker at 37°C for 11 minutes. The trituration and incubation steps were repeated 5 – 7 times until the tissue was completely dissolved. Cells were pelleted at 300 g for 5 minutes, resuspended in DF20 media (Dulbecco's Modified Eagle Medium/ Ham's Nutrient Mixture F12 adjusted to 17 mM $NaHCO_2$ containing 2 mM L-glutamine, 1% P/S and 20% FBS), and preplated for 1 hour to eliminate fibroblasts. Remaining cells were counted using a hemocytometer and plated on glass and plastic surfaces, which were coated with laminin (Sigma-Aldrich; 10 μg/ml in PBS) at room temperature for 1 hour prior to plating. For immunofluorescence analysis, 3×10^5 cells were seeded per well on glass coverslips in 24-well plates. For Western blot analyses of total protein extracts, 5×10^6 cells were seeded in 10 cm-culture dishes. Cells were left undisturbed in DF20 medium at 37°C

for 72 hours, starved overnight with DF medium (Dulbecco's Modified Eagle Medium/ Ham's Nutrient Mixture F12 adjusted to 17 mM $NaHCO_2$ containing 2mM L-glutamine, 1% P/S), and treated in DF medium with recombinant FGF23, FGF2 (both at 100 ng/ml) or AngII (1 μM, Sigma-Aldrich) for 48 hours.

Protein isolation and immunoblotting

HEK293 cells, NRVM or NMVM were treated with growth factors for 30 minutes to analyze activation of signal transduction mediators, or for 48 hours to analyze expression levels of hypertrophic marker proteins. Cells were scraped from 6-well plates using 500 μl CHAPS extraction buffer (20 mM Tris-HCl pH7.5, 500 mM NaCl, 0.5% CHAPS, protease inhibitor cocktail [Roche], protein phosphatase inhibitors [Sigma-Aldrich]) and incubated on ice for 30 minutes. The cell lysate was centrifuged at 14,000 rpm and 4°C for 30 minutes, and the supernatant boiled in sample buffer and analyzed by SDS-PAGE and immunoblotting. For protein extraction from mouse hearts, tissue was isolated, minced and homogenized in RIPA extraction buffer (50 mM Tris-HCl pH 7.5, 200 mM NaCl, 1% Triton X-100, 0.25% DOC, 1mM EDTA, 1 mM EGTA, protease and phosphatase inhibitors) at 1:10 (w:v), and protein lysates were prepared as described above.

Antibodies to β-MHC (NOQ7.5.4D; Sigma-Aldrich; 1:1,000), RCAN1 (rabbit polyclonal, provided by Timothy McKinsey, University of Colorado, Denver, CO (Harrison et al., 2004); 1:1,000), FGFR4 (C-16; Santa Cruz; 1:1,000), total and phospho-ERK1/2 (Cell Signaling; 1:1,000), total and phospho-FRS2α (Santa Cruz 1:1,000; Cell Signaling; 1:1,000), total and phospho-PLCγ (Cell Signaling; 1:1,000), FLAG (M5, Sigma-Aldrich; 1:10,000), V5 (Sigma-Aldrich; 1:10,000) and GAPDH (Abcam; 1:10,000) were used as primary antibodies in

5% milk in TBST (RCAN1, FGFR4, FLAG, V5), 5% BSA in TBST (phospho-FRS2α) or 1.5% FBS in TBS (β-MHC, total and phospho-ERK1/2, total FRS2α, total and phospho-PLCγ, GAPDH) for 1-2 hours. Horseradish peroxidase-conjugated goat-anti-mouse and goat-anti-rabbit (Promega; 1:10,000) were secondary antibodies.

Immunoprecipitation assays

HEK293 cells in 10 cm-dishes were treated with growth factors for 30 minutes, cells were scraped using 1 ml IP buffer (50 mM Tris-HCl pH7.5, 150 mM NaCl, 5 mM $MgCl_2$, 2 mM EGTA, 1% Triton X-100, 5% Glycerol, protease and phosphatase inhibitors), and protein lysates were prepared as described above. V5-tagged proteins were immunoprecipitated using 25 µl of anti-V5 agarose beads (Sigma-Aldrich). After 5 washes in IP buffer, proteins were eluted in 100 µl of sample buffer and analyzed by SDS-PAGE and immunoblotting. For endogenous immunoprecipitation studies from NRVM, cells in 10cm-dishes were treated with growth factors for 30 minutes. Some cells were pre-treated with FGFR4 blocking antibody at 10 µg/ml for 1 hour (human monoclonal, U3-11; U3Pharma). Cells were scraped in 1 ml RIPA buffer, and protein lysates were incubated with 2 µg of anti-FGFR4 (C-16; Santa Cruz) or anti-GFP (Clonetech) as negative control at 4°C under rotation overnight. We added 50 µl of a 1:1 mix of Protein A on sepharose beads and Protein G on agarose beads that were previously equilibrated in RIPA buffer, followed by incubation at 4°C under rotation for 2 hours, protein elution in sample buffer, and SDS-PAGE and Western blot analyses.

RNA isolation and real-time PCR

Total RNA was purified from isolated NRVMs using Trizol (G Biosciences) according to the manufacturer's protocol, and reverse transcribed using Qscript (Quanta Biosciences). Gene expression was quantified by real-time PCR on a Biorad CFX 96 real-time Detection System using 200 ng of cDNA, PerfeCTA SYBR Green FastMix ROX (Quanta Biosciences). RNA from total mouse and rat hearts was extracted using the PureLink RNA Mini Kit (Ambion by Life Technologies) and Trizol (Life Technologies). 2 µg total RNA was reverse-transcribed using First Stand cDNA Synthesis Kit for RT-PCR (AMV) (Roche Diagnostics). Quantitative PCR reactions were carried out in the StepOne plus Real-Time PCR System (Applied Biosystems) using FAST SYBR Green Master Mix (Applied Biosystems). Raw data were quantified via StepOne^{TM} software v2.3 from life Technologies. Relative gene expression was normalized to expression levels of 18S rRNA (for NRVM), and GAPDH or beta actin (mouse and rat tissue), and evaluated using the $2^{-\Delta\Delta Ct}$ method.

In vitro NFAT gene reporter assay

The assay was done as described previously (Kuhn et al., 2009). Briefly, 24 hours after plating, NRVM were serum-starved and infected by an adenovirus (AdNFAT-luc, 20 moi) carrying a firefly luciferase construct under the transcriptional control of three consensus NFAT binding sites (Biomyx). To enable normalization of the ensuing measurements, NRVMs were also infected with an adenovirus (AdRenilla, 10 moi) encoding a renilla luciferase under the transcriptional control of a CMV promoter. Cells were incubated in FGF23 or FGF2 at 25 ng/ml for 2 hours after pre-treatment with or without cyclosporine A (1 µg/ml; Sigma-Aldrich),

AZD4547 (5 nM; ChemieTek), or anti-FGFR4/U3-11 (U3Pharma; 10 μg/ml) for 60 minutes. Chemiluminescence was detected and quantified in $4x10^5$ cells using the Dual-Luciferase Reporter Assay System (Promega) according to the manufacturer's instructions, and Infinite M200 PRO reader (Tecan). Firefly luciferase activities were then normalized to renilla luciferase activities. All experiments were conducted in triplicates and repeated three times.

Isolation of adult murine cardiac myocytes and flow cytometry

Total cardiac cells were isolated from 1-2 month old wild-type mice (n = 3) as described (Kabaeva et al., 2008), and the cell suspension was filtered through a 70 μm strainer. Isolated cells were distributed at 500,000 cells per FACS tube, fixed with 4% PFA at 4°C for 20 minutes, permeabilized with Perm/Wash Buffer (BD Biosciences) at room temperature for 15 minutes, and incubated in 50 μl Perm/Wash Buffer with antibodies against TNNT2 and FGFR4 (Santa Cruz) at 4°C for 1 hour. Cells were washed, incubated with the corresponding Alexa Fluor secondary antibodies at 1:400 in 50 μl Perm/Wash Buffer at 4°C in the dark for 30 minutes, washed again and suspended in 500 μl 1% PFA. Samples were analyzed on a BD LSR Fortessa with a 100 μm-nozzle at high speed running at University of Miami FLOW Lab Core Facility. Raw data was analyzed using FlowJo softare.

Immunostaining of human tissue

Autopsies were conducted in previously healthy individuals who died of accidental, non-cardiac injuries. Tissue specimens from the left ventricle and liver were removed and immediately stored at -80°C. Immunoperoxidase stainings were performed on PFA-fixed, paraffin-embedded, 2 μm-thick tissue sections. For immunofluorescence analysis, deparaffinized

sections were blocked in 3% normal goat serum, 0.3% Triton X-100 in PBS, and incubated with primary mouse monoclonal anti-α-actinin antibody (Sigma-Aldrich) at 40 µg/ml or rabbit polyclonal anti-FGFR4 antibody (C-16; Santa Cruz) at 20 µg/ml in 1% BSA, 0.3% Triton X-100 in PBS, followed by incubation with secondary antibodies coupled to Alexa488 or Atto555 in 1% BSA, 0.3 % Triton X-100 in PBS using MaxBlock autofluorescence reducing reagent kit (Dianova). DAPI (0.2 µg/ml) was used for nuclear staining, and sections were covered with mounting medium (Dako). For immunohistochemistry, tissue was blocked, followed by antigen retrieval with trypsin, and analyzed using rabbit polyclonal antibody against human FGFR4 (C-16; Santa Cruz) at 20 µg/ml in blocking buffer (Universal Elite ABC Kit; Vector Laboratories), followed by incubation with biotinylated secondary horse anti-rabbit antibody, ABC reagent (both Vector Laboratories), and DAB substrate (Sigma-Aldrich) until color development. Tissue was counterstained with Mayer's hematoxylin (Merck), dehydrated through alcohol and subsequently covered with aqueous mounting medium (Roti-Mount; Roth). All images were taken on a Zeiss AxioObserver microscope with a Plan-Apo 63x/N.A. 1.4 oil objective (Carl Zeiss).

Serology

Blood was collected from mice and rats at sacrifice via cardiac puncture and was centrifuged at 4°C and 14,000 rpm for 15 minutes. Serum supernatants were collected, stored at -80°C, and subsequently analyzed in batches for FGF23 (C-terminal assay for mice, intact assay for rats; Immutopics). In mice, serum phosphate and blood urea nitrogen were analyzed by ELISA (Ortho Vitros 250 Chemistry Analyzer). In rats, creatinine and urea nitrogen were measured in 24 hour-urine and blood samples by using an enzymatic assay (Creatinine-Pap, Roche

Diagnostics, Mannheim, Germany) and the urease-GLDH method, respectively (Di Marco et al., 2014). Plasma inorganic phosphate concentration was measured photometrically on a Modular P analyzer (Roche, Mannheim, Germany) using the phosphomolybdate method.

Study Approval

All animal protocols and experimental procedures were approved by the Institutional Animal Care and Use Committees at the University of Miami Miller School of Medicine (high-phosphate diet in wild-type and *FGFR4*$^{-/-}$ mice), the Max Planck Institute for Biochemistry, Martinsried, Germany (*FGFR4Arg385* knock-in mouse), and the University of Münster, Münster, Germany (5/6 nephrectomy in rats). Autopsies and postmortem analyses of human tissue were approved by the medical ethics committee of the Hannover Medical School, Germany.

Supplemental References

Burgess, W.H., Dionne, C.A., Kaplow, J., Mudd, R., Friesel, R., Zilberstein, A., Schlessinger, J., and Jaye, M. (1990). Characterization and cDNA cloning of phospholipase C-gamma, a major substrate for heparin-binding growth factor 1 (acidic fibroblast growth factor)-activated tyrosine kinase. Mol Cell Biol *10*, 4770-4777.

Chen, J., Williams, I.R., Lee, B.H., Duclos, N., Huntly, B.J., Donoghue, D.J., and Gilliland, D.G. (2005). Constitutively activated FGFR3 mutants signal through PLCgamma-dependent and -independent pathways for hematopoietic transformation. Blood *106*, 328-337.

Di Marco, G.S., Reuter, S., Kentrup, D., Grabner, A., Amaral, A.P., Fobker, M., Stypmann, J., Pavenstadt, H., Wolf, M., Faul, C., et al. (2014). Treatment of established left ventricular hypertrophy with fibroblast growth factor receptor blockade in an animal model of CKD. Nephrol Dial Transplant *29*, 2028-2035.

Faul, C., Amaral, A.P., Oskouei, B., Hu, M.C., Sloan, A., Isakova, T., Gutierrez, O.M., Aguillon-Prada, R., Lincoln, J., Hare, J.M., et al. (2011). FGF23 induces left ventricular hypertrophy. J Clin Invest *121*, 4393-4408.

Harrison, B.C., Roberts, C.R., Hood, D.B., Sweeney, M., Gould, J.M., Bush, E.W., and McKinsey, T.A. (2004). The CRM1 nuclear export receptor controls pathological cardiac gene expression. Mol Cell Biol *24*, 10636-10649.

Kabaeva, Z., Zhao, M., and Michele, D.E. (2008). Blebbistatin extends culture life of adult mouse cardiac myocytes and allows efficient and stable transgene expression. Am J Physiol Heart Circ Physiol *294*, H1667-1674.

Kanai, M., Goke, M., Tsunekawa, S., and Podolsky, D.K. (1997). Signal transduction pathway of human fibroblast growth factor receptor 3. Identification of a novel 66-kDa phosphoprotein. J Biol Chem *272*, 6621-6628.

Kreusser, M.M., Lehmann, L.H., Keranov, S., Hoting, M.O., Oehl, U., Kohlhaas, M., Reil, J.C., Neumann, K., Schneider, M.D., Hill, J.A., et al. (2014). Cardiac CaM Kinase II Genes delta and gamma Contribute to Adverse Remodeling but Redundantly Inhibit Calcineurin-Induced Myocardial Hypertrophy. Circulation *130*, 1262-1273.

Kuhn, C., Frank, D., Will, R., Jaschinski, C., Frauen, R., Katus, H.A., and Frey, N. (2009). DYRK1A is a novel negative regulator of cardiomyocyte hypertrophy. J Biol Chem *284*, 17320-17327.

Kurosu, H., Ogawa, Y., Miyoshi, M., Yamamoto, M., Nandi, A., Rosenblatt, K.P., Baum, M.G., Schiavi, S., Hu, M.C., Moe, O.W., et al. (2006). Regulation of fibroblast growth factor-23 signaling by klotho. J Biol Chem *281*, 6120-6123.

Mohammadi, M., Dikic, I., Sorokin, A., Burgess, W.H., Jaye, M., and Schlessinger, J. (1996). Identification of six novel autophosphorylation sites on fibroblast growth factor receptor 1 and elucidation of their importance in receptor activation and signal transduction. Mol Cell Biol *16*, 977-989.

Mohammadi, M., Dionne, C.A., Li, W., Li, N., Spivak, T., Honegger, A.M., Jaye, M., and Schlessinger, J. (1992). Point mutation in FGF receptor eliminates phosphatidylinositol hydrolysis without affecting mitogenesis. Nature *358*, 681-684.

Peters, K.G., Marie, J., Wilson, E., Ives, H.E., Escobedo, J., Del Rosario, M., Mirda, D., and Williams, L.T. (1992). Point mutation of an FGF receptor abolishes phosphatidylinositol turnover and Ca2+ flux but not mitogenesis. Nature *358*, 678-681.

Vainikka, S., Joukov, V., Wennstrom, S., Bergman, M., Pelicci, P.G., and Alitalo, K. (1994). Signal transduction by fibroblast growth factor receptor-4 (FGFR-4). Comparison with FGFR-1. J Biol Chem *269*, 18320-18326.

Vainikka, S., Partanen, J., Bellosta, P., Coulier, F., Birnbaum, D., Basilico, C., Jaye, M., and Alitalo, K. (1992). Fibroblast growth factor receptor-4 shows novel features in genomic structure, ligand binding and signal transduction. EMBO J *11*, 4273-4280.

Wang, J.K., Gao, G., and Goldfarb, M. (1994). Fibroblast growth factor receptors have different signaling and mitogenic potentials. Mol Cell Biol *14*, 181-188.